DOI: 10.1002/anie.201303091

Membrane Proteins

Ligand-Induced Conformational Changes of the Multidrug Resistance Transporter EmrE Probed by Oriented Solid-State NMR Spectroscopy**

*Anindita Gayen, James R. Banigan, and Nathaniel J. Traaseth**

Multidrug resistance (MDR) is a major public health problem that reduces the efficacy of antibiotics in the treatment of infections.[2] One of the most common mechanisms in bacteria for conferring MDR is the coupling of drug efflux with the proton motive force.[3] A prototype for studying ion-coupled active transport is the polytopic *E. coli* membrane protein EmrE, a member of the small multidrug resistance (SMR) family that has 110 residues and four transmembrane (TM) domains. EmrE oligomerizes to form homo-dimers that efflux a wide variety of cations such as ethidium, methyl viologen, and tetraphenylphosphonium (TPP^+).[4] Although controversy still remains in the field,[9] evidence from topology analyses,[5] crystallography,[6] spectroscopy,[7] and molecular modeling[1] support EmrE forming an antiparallel dimer and dual topologies in the cell membrane.[8] Recently, von Heijne and co-workers demonstrated that the anti-parallel state also has higher stability than the parallel form in vivo.[10] Low-resolution structural evidence has defined the general architecture of the anti-parallel quaternary arrangement, which includes cryo-electron microscopy images (7.5 Å × 16 Å)[6a] and an X-ray Cα model of TPP^+ bound EmrE (3.8 Å).[6b] In addition, magic-angle-spinning data for E14[7b] and solution NMR experiments in isotropic bicelles also support the asymmetry of EmrE bound to TPP^+.[7a] The latter study showed monomer interconversion within the dimer, in agreement with an alternating access model of the transporter.[7,11]

The plasticity of the ligand-free or apo EmrE conformation is responsible for adapting to the size and shape of the ligand.[12] Tate and co-workers have previously shown similarity between the apo and TPP^+ bound asymmetric dimer structures, with the latter crystals possessing a higher degree of order.[6a,13] Using the microscopy images, biochemical restraints, and primary sequence conservation data, a backbone structural model was constructed for EmrE bound to TPP^+ (PDB ID: 2I68).[1] The X-ray structure was later reported and is also in qualitative agreement with this model of ligand-bound EmrE.[6b] However, as expected from the experimental resolution of the EmrE crystals, it was not possible to decipher atomic scale details of the structure. To date, no high-resolution structure exists for EmrE in the apo or ligand-bound states. Herein, we offer high-resolution structural insight into the ligand-free form of EmrE in lipid bilayers with the aim of defining the features of this state that are responsible for encoding the molecular recognition mechanism.

Prior to the structural studies, we verified the functionality of our sample preparation using isothermal titration calorimetry (ITC) in 1,2-dimyristoyl-*sn*-glycero-3-phosphocholine (DMPC) lipid vesicles. A dissociation constant for TPP^+ of 46 nM was determined, which corresponds to correctly folded and functional preparations (Supporting Information, Figure S1).[14] Additionally, the fitted stoichiometry revealed a 1:2 TPP^+/monomer ratio, which is consistent with the dimer as the functional oligomeric unit.[4b] To probe the possible parallel or anti-parallel arrangements in the apo form, we carried out cross-linking experiments using a single Cys-mutant of EmrE (S107C) in DMPC liposomes with heterobifunctional (*N*-(ß-maleimidopropyloxy)succinimide ester (BMPS); amine- and thiol-reactive groups) and homofunctional reagents (*N*,*N*′-(*o*-phenylene)dimaleimide (*o*-PDM); thiol reactive groups). Consistent with previous results for TPP^+ bound EmrE,[7a] we observed rapid cross-linking for BMPS between K22 (the only Lys in EmrE) and C107, which is only possible for the anti-parallel dimer arrangement (Figure 1). To the contrary, cross-linking with *o*-PDM was significantly less efficient and dimer formation decreased with increasing lipid to protein ratios (Supporting Information, Figure S2). We found that dimer formation in the presence of BMPS did not significantly change (less than 5%) with the lipid to protein ratio (Figure 1). Our results support the conclusion that it is the interaction between anti-parallel dimers and not the presence of parallel dimers that leads to the observed *o*-PDM cross-linking. These findings for the apo conformation are similar to the single-molecule FRET experiments on TPP^+ bound EmrE that support the anti-parallel configuration of the dimer.[7a]

Does the apo form possess an asymmetric configuration that can be verified at atomic resolution? To answer this, we used oriented solid-state NMR (O-SSNMR) spectroscopy, which is a direct method to probe the structure and tilt angles of membrane proteins relative to the lipid bilayer.[15] EmrE

[*] Dr. A. Gayen, J. R. Banigan, Prof. N. J. Traaseth
Department of Chemistry, New York University
100 Washington Square East, New York, NY 10003 (USA)
E-mail: traaseth@nyu.edu
Homepage: http://www.nyu.edu/fas/dept/chemistry/traasethgroup/

[**] This work was supported by NIH grant K22AI083745 and start-up funds from New York University. We thank Prof. Ray Turner and Dr. Denice Bay for helpful discussions, Tracy Stanzel for technical assistance, the National High Magnetic Field Laboratory for preliminary NMR experiments, and Prof. Bobby Arora and Steve Joy for synthesis of BMPS.

Supporting information for this article (experimental methods) is available on the WWW under http://dx.doi.org/10.1002/anie.201303091.

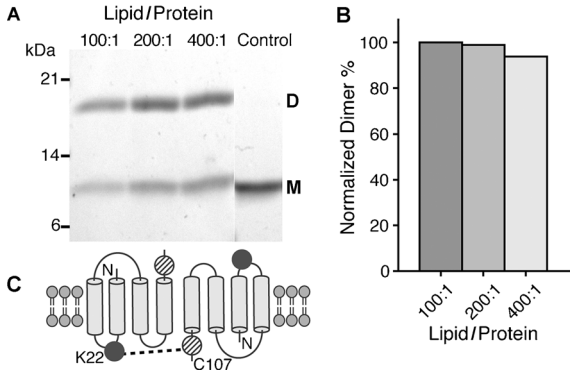

Figure 1. Cross-linking results for the ligand-free form of EmrE in DMPC lipid vesicles. A) SDS-PAGE gel of the BMPS cross-linking reactions with varying lipid/protein ratios having a constant EmrE concentration of 90 μM. B) Normalized dimer formation relative to the 100:1 lipid/protein ratio. C) Scheme of BMPS cross-linking between K22 and C107, which is only possible for the antiparallel topology.

was reconstituted into magnetically aligned bicelles consisting of DMPC/DHPC (1,2-dihexanoyl-*sn*-glycero-3-phosphocholine) in a 3.2:1 molar ratio ($q = 3.2$), similar to the conditions for ITC and cross-linking experiments. The protein alignment in flipped bicelles was checked with 1D $^{1}H/^{15}N$ cross-polarization of [U-^{15}N] labeled EmrE (Supporting Information, Figure S3B). As expected for an aligned protein with short loops and no soluble domains, the ^{15}N chemical shifts were clustered between $\delta = 120$–220 ppm. Because of overlapping resonances in this spectrum, we shifted our attention to selectively labeled samples ([^{15}N-Val] and [^{15}N-Met]) that gave local probes distributed in each of the TM domains (Figure 2): TM1 (V15, M21), TM2 (V34), TM3 (V66, V69), and TM4 (M91, M92, V98).

A sensitivity-enhanced version[16] of PISEMA[17] was recorded for each sample to correlate ^{15}N anisotropic chemical shifts with ^{1}H–^{15}N dipolar couplings. The PISEMA spectrum for [^{15}N-Val] apo EmrE revealed ten resolved peaks having chemical shifts corresponding to TM domain helices

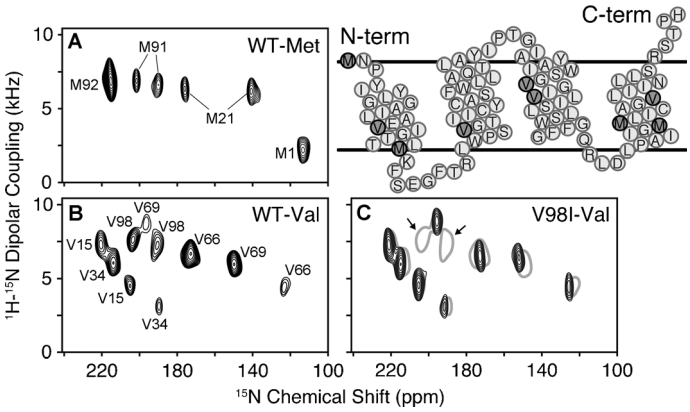

Figure 2. PISEMA spectra of ligand-free EmrE in flipped magnetically aligned bicelles (DMPC/DHPC, 3.2:1). A) [^{15}N-Met] and B) [^{15}N-Val] wild-type EmrE PISEMA spectra. C) [^{15}N-Val] V98I EmrE PISEMA (black) showing two less peaks than in the wild-type spectrum (gray). The arrows indicate peaks corresponding to V98.

(Figure 2B). Interestingly, this is twice the expected number of Val residues in the primary sequence and shows there are two populations with different angular dependencies with respect to the lipid bilayer normal. Similar to the Val spectrum, the experiment on [^{15}N-Met] EmrE in Figure 2A also showed peak doubling for M21 and M91. The lack of doubling for M1 and M92 is due to the location at the dynamic N-terminus and the presence of overlapping populations, which is evident by the twofold greater peak intensity of M92 with respect to M21 or M91. Taken together with our ITC and cross-linking results, the data strongly support the conclusion that the two asymmetric populations have different tilt angles with respect to the membrane and stem from the anti-parallel quaternary arrangement of the apo dimer.

To extract meaningful structural restraints, assignment of the PISEMA spectra was carried out. This is typically achieved by selective isotope labeling in conjunction with the assumption of periodic spectral patterns (PISA wheels)[18] and the use of spin diffusion techniques.[19] While somewhat straightforward for a single helix, polytopic membrane proteins present increased challenges that result from overlapping spectra. In fact, for the asymmetric EmrE dimer, this involves eight PISA wheels. Therefore, as an alternative, we implemented a mutagenesis approach to assign the spectra in Figure 2. All single-site mutations preserved the approximate size and hydrophobicity of the wild-type residue (Val and Met to Ile), and importantly did not disrupt the binding affinity or stoichiometry to TPP^{+} (Supporting Information, Table S1). An example of this assignment approach is shown for [^{15}N-Val] V98I EmrE, which has eight resolved peaks that overlap with eight of the ten peaks in the corresponding wild-type [^{15}N-Val] spectrum (Figure 2C). This experiment, along with other spectra of mutant proteins (Supporting Information, Figure S4), confirmed the two populations and provided an unambiguous way to assign the PISEMA spectra. The mutagenesis approach to assign the peaks cannot directly distinguish between monomers A and B for each residue, rather these assignments were obtained from the qualitative agreement between the observed PISEMA profile and those values calculated from the computational structure 2I68 (Supporting Information, Figure S5). Future work will seek to assign the peaks to specific monomers without assistance from an existing model.

What is the effect of ligand binding on the asymmetric apo EmrE conformation? To provide insight, we carried out a titration with TPP^{+} and monitored the spectral changes using PISEMA spectroscopy. Upon addition of one-half molar equivalent TPP^{+} relative to the EmrE dimer concentration, we observed additional peak splitting in the slow chemical exchange timescale for several residues (Figure 3B). The slow exchange between peaks with equal intensity is consistent with the nanomolar binding affinity to TPP^{+} (i.e., 50% free and 50% bound dimers). We then made a saturating addition of ligand to the same sample and observed eight clearly distinguishable peaks, which was the same number as the initial ligand-free spectrum. These data are evidence for a specific rearrangement of the transporter upon ligand binding and also validate the two asymmetric populations we

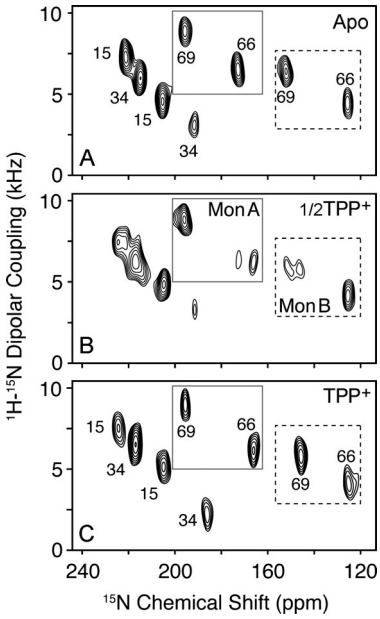

Figure 3. TPP^{+} titration of EmrE probed with PISEMA spectroscopy. A) Ligand-free spectrum of [^{15}N-Val] V98I, B) 0.5 molar equivalents TPP^{+} relative to the dimer, and C) a saturating addition of ligand to the same sample. 1D slices are shown in the Supporting Information, Figure S8.

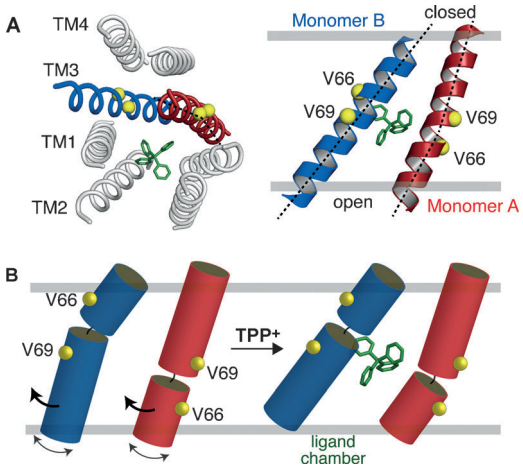

Figure 4. Bending motion of EmrE TM3. A) Computational model of EmrE by Fleishman et al.[1] showing the kink in monomer A of PDB 2I68. B) Scheme of TM3 bending motion consistent with the differential behavior of V66 and V69 in monomers A and B in the PISEMA spectra shown in Figure 3.

observed in the apo form. The changes that occurred to Met residues upon TPP^{+} binding are shown in the Supporting Information, Figure S6. Although we observed chemical shift perturbations in each TM domain (Supporting Information, Figure S7 A), one of the key features of the spectra is the differential behavior found for V66 and V69 within the same monomer (Figure 3; Figure S8). The fact that one peak showed a chemical shift perturbation and the other did not is suggestive of a structural rearrangement involving helix bending around G67 in TM3 (sequence is G65-V66-G67-I68-V69). This conclusion is consistent with the computational model of EmrE having a discernible kink between V66 and V69 in TM3 of monomer B[1] and EPR paramagnetic accessibility experiments in liposomes.[12b] Note that all other helices in the computational model were ideal, with no major deviations from uniform dihedral angles. In Figure 4, we depict the changes in TM3 upon binding to TPP^{+}. In this model, the N-terminal half of monomer A and the C-terminal side of monomer B tilt in response to ligand binding, which is consistent with our experimental PISEMA spectra.

The combination of O-SSNMR and cross-linking experiments demonstrated that the ligand-free form of EmrE is an anti-parallel dimer with asymmetric tilt angles relative to the lipid bilayer normal. This asymmetry is particularly unusual given the fact that nearly all homo-oligomeric proteins found in biology possess symmetry, which has been argued to enhance stability and allosteric control over assemblies.[21] Our atomic-resolution observations were possible with PISEMA spectroscopy and further validate the backbone structural models available from cryo-electron microscopy and X-ray crystallography.[6b,13] Nevertheless, the PISEMA spectra showed quantitative differences with the structural models and spectral perturbations between the apo and TPP^{+} bound forms that were not easily discernible in the cryo-electron microscopy images (Supporting Information, Figure S7).[13] One example is the fact that the fitted rotation angles from the PISEMA data for TM4 differed by approximately 33° and 50° in monomers A and B with respect to those in PDB 2I68 (Supporting Information, Figures S9,S10). These subtle atomic-scale differences emphasize the need for a high-resolution structure of the apo and ligand-bound forms of EmrE to fully understand the molecular recognition and transport mechanisms within the lipid membrane.[20] Because the MDR phenomenon hinges on the recognition of a wide variety of ligands, studies that give additional insight into the structural plasticity of apo EmrE are of paramount importance.

Received: April 12, 2013
Revised: July 12, 2013
Published online: August 12, 2013

Keywords: EmrE · membrane proteins · multidrug resistance · NMR spectroscopy · oriented solid-state NMR

[1] S. J. Fleishman, S. E. Harrington, A. Enosh, D. Halperin, C. G. Tate, N. Ben-Tal, *J. Mol. Biol.* **2006**, *364*, 54–67.
[2] H. Nikaido, *Annu. Rev. Biochem.* **2009**, *78*, 119–146.
[3] C. F. Higgins, *Nature* **2007**, *446*, 749–757.
[4] a) D. C. Bay, R. J. Turner, *BMC Evol. Biol.* **2009**, *9*, 140; b) S. Schuldiner, *Biochim. Biophys. Acta Proteins Proteomics* **2009**, *1794*, 748–762.
[5] M. Rapp, S. Seppala, E. Granseth, G. von Heijne, *Science* **2007**, *315*, 1282–1284.
[6] a) I. Ubarretxena-Belandia, J. M. Baldwin, S. Schuldiner, C. G. Tate, *EMBO J.* **2003**, *22*, 6175–6181; b) Y. J. Chen, O. Pornillos, S. Lieu, C. Ma, A. P. Chen, G. Chang, *Proc. Natl. Acad. Sci. USA* **2007**, *104*, 18999–19004.

[7] a) E. A. Morrison, G. T. DeKoster, S. Dutta, R. Vafabakhsh, M. W. Clarkson, A. Bahl, D. Kern, T. Ha, K. A. Henzler-Wildman, *Nature* **2012**, *481*, 45 – 50; b) I. Lehner, D. Basting, B. Meyer, W. Haase, T. Manolikas, C. Kaiser, M. Karas, C. Glaubitz, *J. Biol. Chem.* **2008**, *283*, 3281 – 3288.
[8] M. Rapp, E. Granseth, S. Seppala, G. von Heijne, *Nat. Struct. Mol. Biol.* **2006**, *13*, 112 – 116.
[9] S. Schuldiner, *Trends Biochem. Sci.* **2012**, *37*, 215 – 219.
[10] P. Lloris-Garcera, F. Bianchi, J. S. Slusky, S. Seppala, D. O. Daley, G. von Heijne, *J. Biol. Chem.* **2012**, *287*, 26052 – 26059.
[11] H. Yerushalmi, S. Schuldiner, *Biochemistry* **2000**, *39*, 14711 – 14719.
[12] a) M. V. Korkhov, C. G. Tate, *J. Mol. Biol.* **2008**, *377*, 1094 – 1103; b) S. T. Amadi, H. A. Koteiche, S. Mishra, H. S. McHaourab, *J. Biol. Chem.* **2010**, *285*, 26710 – 26718.
[13] C. G. Tate, E. R. Kunji, M. Lebendiker, S. Schuldiner, *EMBO J.* **2001**, *20*, 77 – 81.
[14] C. G. Tate, *Curr. Opin. Struct. Biol.* **2006**, *16*, 457 – 464.
[15] a) M. Sharma, M. Yi, H. Dong, H. Qin, E. Peterson, D. D. Busath, H. X. Zhou, T. A. Cross, *Science* **2010**, *330*, 509 – 512; b) A. A. De Angelis, S. C. Howell, A. A. Nevzorov, S. J. Opella, *J. Am. Chem. Soc.* **2006**, *128*, 12256 – 12267; c) N. J. Traaseth, L. Shi, R. Verardi, D. G. Mullen, G. Barany, G. Veglia, *Proc. Natl. Acad. Sci. USA* **2009**, *106*, 10165 – 10170.
[16] T. Gopinath, G. Veglia, *J. Am. Chem. Soc.* **2009**, *131*, 5754 – 5756.
[17] C. H. Wu, A. Ramamoorthy, S. J. Opella, *J. Magn. Reson.* **1994**, *109*, 270 – 272.
[18] a) F. M. Marassi, S. J. Opella, *J. Magn. Reson.* **2000**, *144*, 150 – 155; b) J. Wang, J. Denny, C. Tian, S. Kim, Y. Mo, F. Kovacs, Z. Song, K. Nishimura, Z. Gan, R. Fu, J. R. Quine, T. A. Cross, *J. Magn. Reson.* **2000**, *144*, 162 – 167.
[19] a) R. W. Knox, G. J. Lu, S. J. Opella, A. A. Nevzorov, *J. Am. Chem. Soc.* **2010**, *132*, 8255 – 8257; b) K. R. Mote, T. Gopinath, N. J. Traaseth, J. Kitchen, P. L. Gor′kov, W. W. Brey, G. Veglia, *J. Biomol. NMR* **2011**, *51*, 339 – 346; c) J. Xu, J. Struppe, A. Ramamoorthy, *J. Chem. Phys.* **2008**, *128*, 052308; d) N. J. Traaseth, T. Gopinath, G. Veglia, *J. Phys. Chem. B* **2010**, *114*, 13872 – 13880.
[20] J. R. Banigan, A. Gayen, N. J. Traaseth, *J. Biomol. NMR* **2013**, *55*, 391 – 399.
[21] D. S. Goodsell, A. J. Olson, *Annu. Rev. Biophys. Biomol. Struct.* **2000**, *29*, 105 – 153.

